

An FPGA-based Technique for Linearizing RF Power Amplifiers

Mohammad Reza Mahmoodi and Zahra Fahimi

Department of Electrical and Computer Engineering

University of California Santa Barbara, Santa Barbara, CA 93106, USA

**Corresponding author's E-mail: mr.mahmoodi@umail.ucsb.edu*

Abstract

In this paper, an efficient predistortion method for linearization of RF power amplifiers is proposed. In this technique, appropriate signals are added to the main baseband input signal to reduce the nonlinearity of the PA. The non-linear relationship between input and output of an RF PA is analyzed and optimum values for the injection signals at the intermodulation frequencies are obtained. In addition, a high-speed low-cost MATLAB-FPGA interface is designed that can be used both in the training and testing phases of the system. Simulation results indicate that the proposed technique is capable of remarkably reducing spectral regrowth in adjacent channels for different non-constant envelope signals. Using a QPSK signal, the spectral regrowth and ACPR of the PA are decreased by 20dB and 26dB, respectively.

Keywords: *Linearization, Power Amplifier, Injection, IMD, IM3 Cancellation, FPGA*

1-Introduction

RF power amplifier (PA) is an integral part in transmit chain of a transceiver. A PA increases the power level of the RF signal in order to meet the minimum required RF coverage range of the transmitter. Among different challenges in the design of an RF PA, achieving both high linearity and high efficiency is a critical one. The efficiency can be increased if the active devices used in the PA operate as switches whose strong nonlinearity behavior causes severe distortion on the envelope of the output signal. This distortion results in spectral regrowth that can lead to interference with adjacent channels and thus increases the bit error rates of the transmitted data. In modern wireless communication systems, non-constant envelope signals such as M-QAM, QPSK, etc. are utilized to improve spectrum efficiency and the channel capacity in an optimum way. The high peak to average power ratio (PAPR) in these modulations necessitates using a linear PA to follow the envelope variations of the RF signal. Therefore, the linearization issue becomes extremely crucial and important. A PA with enhanced linearity can operate near its compression point that leads to the higher power efficiency of the amplifier. In recent years, many linearization techniques such as feedback [1], feedforward [2], analog predistortion [3] and digital predistortion (DPD) [4] have been proposed. The first method i.e., feedback, is based on the idea of comparing the input signal with the distorted output signal. Using a negative feedback loop and correcting the input signal according to the result of comparison, the linearity is improved to some extent. Different related configurations such as RF feedback, active RF feedback, distortion feedback and modulation feedback are already presented in the literature. One disadvantage of using feedback mechanism is the lack of robustness with respect to the parameters' variations since the resulted responses might be unstable. Feedforward is another technique in which the distortion components are extracted and subtracted from the output signal. This technique uses an additional amplifier to manipulate the output from the PA.

Among various reported linearization techniques, predistortion is relatively simple and low cost. The idea is to extract PA model and leverage a reverse system in front of the PA in order to cancel the total distortion exerted to the input signal. A variety of techniques including analog and digital predistortion have been already presented. In the case of analog predistortion, the inverse AM/AM and AM/PM characteristics are employed to construct the predistorter. In case of DPD techniques, the predistortion characteristic is created by using digital components and DSP operations. One of the most recently developed predistortion methods in the baseband digital predistortion is the injection technique. The main idea is to add controlled signals to the baseband signal and eliminate the distortion. Relatively smaller size, low cost, simplicity of realization and efficiency are main advantages of the injection method. However this method also has its own drawbacks. For instance, the extra injected components that are used to compensate the original distortions may produce other distortions spurs, which limits the PA performance.

In this paper, an analytical description for injection in IMD (Inter-modulation Distortion) frequency (a.k.a. third order injection) in two cases of two-tone and wideband signal is proposed and a relationship between injected and output IMD products is developed. After measuring the amplitude and phase of original IMD for a class-A power amplifier, the appropriate and optimum baseband injection signals are derived. The injection signal is added to the baseband input signal and the combined signal is applied to the PA through an up-converter mixer. Using this predistortion procedure, we can significantly reduce the IMD components of the output signal. The analysis of the relationship between the distorted and input signals and also optimized calculations related to the injected signals are described. A FPGA-based system is also developed in order to implement this method. The obtained results are comparable with those of state-of-the art methods. The rest of the paper is organized as follows. The proposed method is explained in section II. Section III presents the simulation results and in Section IV, the FPGA implementation is elucidated. Finally, conclusion is provided in Section V.

2- The Proposed Method

The input-output relationship of a nonlinear PA can be written as [5]:

$$V_{out}(t) = g_1 V_{in} + g_2 V_{in}^2 + g_3 V_{in}^3 + \dots \quad (1)$$

where $V_{in}(t)$ is the input signal and g_i is the coefficient of the i^{th} nonlinear term. $V_{in}(t)$ is a modulated signal with amplitude and phase of $V(t)$ and $\phi(t)$, respectively:

$$V_{in}(t) = V(t) \cos(\omega t + \phi(t)) \quad (2)$$

Rewriting (2) in terms of in-phase and quadrature phase components, i.e., I and Q, we get:

$$V_{in}(t) = V_s(t)(I \cos(\omega t) + Q \sin(\omega t)) \quad (3)$$

where $V_s \triangleq V/\sqrt{I^2 + Q^2}$ and I and Q are defined as follows:

$$I = \frac{V(t)}{V} \cos(\phi(t)) , \quad Q = \frac{V(t)}{V} \sin(\phi(t)) \quad (4)$$

Substituting (3) in (1) and ignoring the terms above the third one, we can obtain the output voltage at the fundamental frequency as:

$$V_{out_{fund}}(t) = g_1 V_s(t)(I \cos(\omega t) + Q \sin(\omega t)) + \frac{3}{4} g_3 V_s^3(t)(I^2 + Q^2)(I \cos(\omega t) + Q \sin(\omega t)) \quad (5)$$

where the first term is the linear term with the gain of g_1 and the second term is the distortion component due to the third order term. The idea of injection is to add an extra signal at two lower and upper third order intermodulation frequencies to the main input signal in order to compensate the distortion products [6]. The compensation can be done by applying the injection signal at difference frequency [7] or at second harmonic frequency [8]. In fact, the idea is to inject the signal in such a way

that it can eliminate the harmonic distortion product at particular frequency. While applying an appropriate injection signal can significantly reduce the distortion, using an injection signal with improper amplitude and phase may cause more nonlinearity behavior in the PA [9]. The injection signal could be added to the two main tones at the frequencies of lower and upper IM3s.

To explain the mathematical description of the proposed method, a two-tone signal is considered as the input.

$$V_{in}(t) = V_s(\cos(\omega_1 t) + \cos(\omega_2 t)) \quad (6)$$

When this signal is applied to a nonlinear PA, different IMD components are produced in the lower and upper sides of the main two tones. By substituting (6) in (1), we can obtain the output voltage relationship as:

$$V_{out}(t) = g_1 V_s(\cos(\omega_1 t) + \sin(\omega_2 t)) + g_2 V_s^2(\cos(\omega_1 t) + \sin(\omega_2 t))^2 + g_3 V_s^3(\cos(\omega_1 t) + \sin(\omega_2 t))^3 \quad (7)$$

The frequency components that are produced by the third order term in (7) can be written as:

$$V_{out,IM3}(t) = V_{3\omega_1} \cos(3\omega_1 t) + V_{3\omega_2} \cos(3\omega_2 t) + V_{2\omega_1-\omega_2} \cos((2\omega_1 - \omega_2)t) + V_{2\omega_2-\omega_1} \cos((2\omega_2 - \omega_1)t) + V_{2\omega_1+\omega_2} \cos((2\omega_1 + \omega_2)t) + V_{2\omega_2+\omega_1} \cos((2\omega_2 + \omega_1)t) \quad (8)$$

Among different terms only $V_{2\omega_1-\omega_2}$ and $V_{2\omega_2-\omega_1}$ are placed in the PA bandwidth and thus for canceling the distortion components, two signals with proper amplitudes and phases are injected at frequencies $2\omega_1-\omega_2$ and $2\omega_2-\omega_1$ where IM3L and IM3U are placed, respectively. Lower and upper IM3 components at the output as a result of applying both injection signals and PA nonlinearity are given by:

$$\begin{bmatrix} O_{IM3L} \\ O_{IM3U} \end{bmatrix} = \begin{bmatrix} a_{11} & 0 \\ 0 & a_{22} \end{bmatrix} \cdot \begin{bmatrix} I_{IM3L} \\ I_{IM3U} \end{bmatrix} + \begin{bmatrix} IM3L \\ IM3U \end{bmatrix} \quad (9)$$

where O_{IM3L} and O_{IM3U} denote the output values of the PA at IM3 frequencies, I_{IM3L} and I_{IM3U} are the injection signals at $2\omega_1-\omega_2$ and $2\omega_2-\omega_1$, the elements of the gain matrix, i.e., a_{11} and a_{22} represent the linear gains for the injection signals, and IM3L and IM3U are the lower and upper third order intermodulation spurs respectively. Note that the magnitude of the injection signals is relatively small and thus it is assumed that the PA behaves linearly in response to these signals. Each of the aforementioned parameters can be expressed in the polar form as:

$$I_{IM3L} = i_1 \cdot e^{j\phi_1}, \quad I_{IM3U} = i_2 \cdot e^{j\phi_2} \quad (10)$$

$$O_{IM3L} = o_1 \cdot e^{j\theta_1}, \quad O_{IM3U} = o_2 \cdot e^{j\theta_2} \quad (11)$$

$$a_{11} = a_1 \cdot e^{j\phi_1}, \quad a_{22} = a_2 \cdot e^{j\phi_2} \quad (12)$$

To completely eliminate IM3s at the output, eq. (9) should be made equal to zero:

$$\begin{bmatrix} 0 \\ 0 \end{bmatrix} = \begin{bmatrix} a_{11} & 0 \\ 0 & a_{22} \end{bmatrix} \cdot \begin{bmatrix} I_{IM3L} \\ I_{IM3U} \end{bmatrix} + \begin{bmatrix} IM3L \\ IM3U \end{bmatrix} \quad (13)$$

Given the gain matrix and IM3 spurs, the proper injection signal could be obtained by:

$$\begin{bmatrix} I_{IM3L} \\ I_{IM3U} \end{bmatrix} = - \begin{bmatrix} a_{11} & 0 \\ 0 & a_{22} \end{bmatrix}^{-1} \cdot \begin{bmatrix} IM3L \\ IM3U \end{bmatrix} \quad (14)$$

By deriving the mathematical relationship between input and output signals at IM3 frequencies, appropriate values for amplitude and phase of the injection signals are obtained. In the absence of the main two tone signals, when only the injection signals are applied to the PA, the PA output is given by:

$$\begin{bmatrix} O_{3L} \\ O_{3U} \end{bmatrix} = \begin{bmatrix} a_{11} & 0 \\ 0 & a_{22} \end{bmatrix} \cdot \begin{bmatrix} I_{3L} \\ I_{3U} \end{bmatrix} \quad (15)$$

Input signals I_{3L} and I_{3U} with known magnitude and phase at $2\omega_1 - \omega_2$ and $2\omega_2 - \omega_1$ are applied to the PA and the linear response of the PA is measured at its output. Thus:

$$a_{11} = \frac{O_{3L}}{I_{3L}} \quad , \quad a_{22} = \frac{O_{3U}}{I_{3U}} \quad (16)$$

When two main tones with both lower and upper IM3 injection signals are simultaneously applied to the PA, due to the nonlinear behavior of the PA for the main tones, IM3 components at $2\omega_1 - \omega_2$ and $2\omega_2 - \omega_1$ are produced. In the presence of main tones and two IM3 injection signals, mixing action between each IM3 and higher order harmonics of main tones results in extra spurs at $2\omega_1 - \omega_2$ and $2\omega_2 - \omega_1$. For instance, harmonics $m\omega_1$ and $n\omega_2$ can be mixed with lower third order intermodulation, $(2\omega_1 - \omega_2)$, in such a way that it produces a new spur at the upper third order intermodulation, $(2\omega_2 - \omega_1)$. In this case, Eq. (17) should be satisfied:

$$2\omega_1 - \omega_2 + m\omega_1 + n\omega_2 = 2\omega_2 - \omega_1 \quad (17)$$

Eq. (17) shows that how the PA nonlinearity causes interaction between lower and upper IM3s in the presence of the main tones. By equating the corresponding factors of ω_1 and ω_2 on two sides in (17), we get $m=-3$ and $n=+3$. This means that the third harmonics of two tones through intermodulation with each IM3 components produces new spur at the other IM3 frequency. For example, Eq. (17) proves that lower IM3 produces an extra spur at the upper IM3, and vice versa. As a result, when both of IM3 injection signals with two main tones are applied, the new produced IM3s degrade the linearity performance of the PA. By including the interaction effect Eq. (9) can be written as:

$$\begin{bmatrix} O_{IM3L} \\ O_{IM3U} \end{bmatrix} = \begin{bmatrix} a_{11} & a_{12} \\ a_{21} & a_{22} \end{bmatrix} \cdot \begin{bmatrix} I_{IM3L} \\ I_{IM3U} \end{bmatrix} + \begin{bmatrix} IM3L \\ IM3U \end{bmatrix} \quad (18)$$

where nonzero entries of a_{12} and a_{21} are added to consider the interaction of two lower and upper IM3s on each other.

A wideband signal in the frequency domain is regarded as a number of tones in an specific bandwidth. When a wideband signal is applied to a PA, in addition to amplifying the main channel, many other tones are generated in lower and upper side bands of the output signal. But, they have small amplitude in compare with main channel tones. The generated tones named distortions due to the PA nonlinearities cause spreading signal into adjacent channels. The same procedure used for two tones can be generalized for wideband signals to eliminate distortions in sidebands. Assuming the wideband signal consists of "n" different frequency samples, Eq. (9) is extended to higher order matrix relationship as below:

$$\mathbf{O} = \mathbf{A} \mathbf{I} + \mathbf{IM3} \quad (19a)$$

$$\begin{bmatrix} O_{1_{IM3L}} \\ \vdots \\ O_{n_{IM3L}} \\ O_{1_{IM3U}} \\ \vdots \\ O_{n_{IM3U}} \end{bmatrix} = \begin{bmatrix} a_{11} & 0 & 0 & 0 & 0 \\ 0 & a_{22} & 0 & 0 & 0 \\ 0 & 0 & \cdot & 0 & 0 \\ 0 & 0 & 0 & \cdot & 0 \\ 0 & 0 & 0 & 0 & a_{2n2n} \end{bmatrix} \cdot \begin{bmatrix} I_{1_{IM3L}} \\ \vdots \\ I_{n_{IM3L}} \\ I_{1_{IM3U}} \\ \vdots \\ I_{n_{IM3U}} \end{bmatrix} + \begin{bmatrix} IM3L_1 \\ \vdots \\ IM3L_n \\ IM3U_1 \\ \vdots \\ IM3U_n \end{bmatrix} \quad (19b)$$

Here, the dimension of vectors \mathbf{O} , \mathbf{I} and $\mathbf{IM3}$ is $2n \times 1$ and that of matrix \mathbf{A} is $2n \times 2n$. First, the linear gain of the PA (entries of matrix \mathbf{A}) and IM3 components created by different samples of the main input signals (elements of vector $\mathbf{IM3}$) are obtained. The proper injection signals for lower and upper sidebands are calculated further:

$$\begin{bmatrix} I_{1_IM3L} \\ \vdots \\ I_{n_IM3L} \\ I_{1_IM3U} \\ \vdots \\ I_{n_IM3U} \end{bmatrix} = - \begin{bmatrix} a_{11} & 0 & 0 & 0 & 0 \\ 0 & a_{22} & 0 & 0 & 0 \\ 0 & 0 & \cdot & 0 & 0 \\ 0 & 0 & 0 & \cdot & 0 \\ 0 & 0 & 0 & 0 & a_{2n2n} \end{bmatrix}^{-1} \begin{bmatrix} IM3L_1 \\ \vdots \\ IM3L_n \\ IM3U_1 \\ \vdots \\ IM3U_n \end{bmatrix} \quad (20)$$

In order to calculate the injection signals, it is necessary to measure the linear gain of the PA for each injection signal. Supposing the limited number of sub-frequencies in the lower and upper sidebands, arbitrary amplitudes and phases for injection signals in the first round are considered. Then, the outputs of the PA in response to the injected signals are measured and the linear gain of the PA is calculated from:

$$\begin{bmatrix} O_{1_3L} \\ \vdots \\ O_{n_3L} \\ O_{1_3U} \\ \vdots \\ O_{n_3U} \end{bmatrix} = \begin{bmatrix} a_{11} & 0 & 0 & 0 & 0 \\ 0 & a_{22} & 0 & 0 & 0 \\ 0 & 0 & \cdot & 0 & 0 \\ 0 & 0 & 0 & \cdot & 0 \\ 0 & 0 & 0 & 0 & a_{2n2n} \end{bmatrix} \cdot \begin{bmatrix} I_{1_3L} \\ \vdots \\ I_{n_3L} \\ I_{1_3U} \\ \vdots \\ I_{n_3U} \end{bmatrix} \quad (21)$$

Given the linear gain of PA, the desired injection signal is calculated using Eq. (24). Considering the interaction effect in the presence of the main input signal (23b) is changed to:

$$\begin{bmatrix} O_{1_IM3L} \\ \vdots \\ O_{n_IM3L} \\ O_{1_IM3U} \\ \vdots \\ O_{n_IM3U} \end{bmatrix} = \begin{bmatrix} a_{11} & 0 \dots \dots & \dots 0 & a_{1,n+1} & \dots \dots & a_{1,2n} \\ 0 & \ddots & \dots 0 & \vdots & \ddots & \vdots \\ 0 & \dots \dots 0 & a_{nn} & a_{n,n+1} & \dots \dots & a_{nn} \\ a_{n+1,1} & \dots \dots & a_{n+1,n} & a_{n+1,n+1} & 0 \dots & \dots 0 \\ \vdots & \ddots & \vdots & 0 & \ddots & \dots 0 \\ a_{2n,1} & \dots \dots & a_{nn} & \vdots & \dots 0 & a_{2n2n} \end{bmatrix} \times \begin{bmatrix} I_{1_IM3L} \\ \vdots \\ I_{n_IM3L} \\ I_{1_IM3U} \\ \vdots \\ I_{n_IM3U} \end{bmatrix} + \begin{bmatrix} IM3L_1 \\ \vdots \\ IM3L_n \\ IM3U_1 \\ \vdots \\ IM3U_n \end{bmatrix} \quad (22)$$

where a_{ij} with $i \neq j$ is the effect of $IM3U_j$ on $IM3L_i$ and a_{ji} is the effect of $IM3L_i$ on $IM3U_j$. Noteworthy, calculating the a_{ij} requires specific coding techniques with regard to both high dimensions of the matrixes and relatively pretty diminutive values.

3- Simulation Environment

A cascode 2.5 GHz class-A power amplifier with 15dB power gain is designed to demonstrate the performance of the proposed baseband injection technique. Two thick oxide NMOS transistors from a 0.18 μ m CMOS technology have been used. The whole system including the RF power amplifier is shown in Fig. 1. The third order intermodulation spurs generated due to the nonlinearity of the PA for each sample are measured and after down-converting sent through the lower branch to form the $\mathbf{IM3}$ vector in (19b). In the following, PA's linear response is obtained for the injection signals at lower and upper IM3 frequencies. With this end in view, many different samples at these frequencies are applied to the PA through the upper branch and their corresponding responses are measured and saved. The elements of the matrix \mathbf{A} are the PA response to different injection signals at IM3L and IM3U frequencies. The

main diagonal elements of this matrix specify the linear response of the PA to each individual IM3 injection signal while the off-diagonal entries represent the reciprocal interaction of each IM3 spur on the other one. For example entry a_{ij} shows how the j^{th} input injection signal affects i^{th} spur at the output. Multiplication of the inverse of \mathbf{A} by the vector $\mathbf{IM3}$ gives the proper injection signals. Finally, the vector \mathbf{I} is added to the main input signal to eliminate the extra IM3 spurs due to the PA nonlinearity. Fig. 2 shows the output spectrum with and without applying third order injection signals for 16QAM. The ACPR is reduced more than 21dB, 21.5dB, and 26dB for 16QAM, 64QAM, and QPSK modulation, respectively.

As discussed earlier the proper injection signals are obtained based on the PA response to the IM3 and main input tones. This means that any change in the PA parameters due to either temperature or process will affect the results. In conclusion, applying a specific injection signal to the PA input while the PA characteristic has been changed due to process variations not only will not improve the nonlinearity but it may make the situation worse.

In case of FPGA implementation of the predistortion system, this problem is not critical as online adaptive learning is exploited; hence, the performance will not degrade. However, if injection signals are integrated within the RF PA (on-chip), then the solution is to individually extract the PA characteristic for different process corners and saving the corresponding signals in separate lookup tables. Then with the aid of a circuit that can distinguish each process corner, an appropriate injection signal is selected and applied to the PA. Citing an example, the circuit in Fig. 3 could be utilized for the purpose. The gate-source voltage of M_0 changes with process variations so that it has its maximum value for slow-slow and minimum value in fast-fast case. By comparing the gate-source voltage with two stable reference voltages, a two-bit control signal is produced. Three separate lookup tables which contain the predistortion data for three different corners are addressed by two bits b_1 and b_0 . The output spectrum of the PA for a 16QAM input signal in FF corner was calculated and it has been observed when a proper injection signal is applied to the PA, ACPR is improved independent of process variations. Noteworthy, this idea could be simply extended to achieve higher accuracies by employing more tables with moderate process variations. Noteworthy, the simulation results also demonstrate that temperature variations from -40C to +125C have no considerable effect on ACPR.

4- FPGA Implementation

A high-speed low-cost hardware framework based on MATLAB-FPGA interface is proposed that can be used in many applications [10] including the training and testing of this system. In MATLAB, a UDP data management core is programmed to communicate with the FPGA via Gigabit Ethernet connection. In hardware, the structure is based on dynamic data transmission between the UDP stack, memory controller and DSP modules. UDP stack manages the external send and receive communication tasks while the off-chip DDR3 memory is utilized in buffering data whenever it is necessary (Fig. 4).

MATLAB initiates the entire operation. The DSP system Toolbox is utilized in order to provide a UDP/IP data packets out of digital signal. In the FPGA, input packets are received and depend on the content of the data, a decision will be taken. This is mainly due to the fact that there are two standard protocols utilized here. The first one is ARP (address resolution protocol) and the other one is the UDP which carries the main data. The former one is prerequisite in order to establish the connection and the latter one is used for data transferring.

The overall operation of the system is divided into two parts. One is a training phase which in order to obtain injection signals, the output signal is provided to the MATLAB either by the FPGA itself or an external device such as a HP8751A network analyzer. By providing output samples of the PA for MATLAB, injection signal will be calculated as it was discussed in former sections. The second part is testing phase in which the data i.e. injection signal, which will be downloaded to the external SDRAM thorough the FPGA, and then will be sent to the output interface and the transmitter chain. The whole procedure is controlled by MATLAB and FPGA push button keys. The main challenge is the design of UDP stack and MCB interfaces which is briefly explained further.

Assume that the injection signal is already calculated in MATLAB by employing a power amplifier. Here, the goal is to transfer data into the FPGA and the high dense SDRAM followingly. Subsequently, the data is read from the high performance SDRAM and sent to the transmitter chain by the FPGA in main operation. The operation starts by loading data into the FPGA and probably its storage in an off-chip high dense SDRAM. Most DSP applications require large memories for storage and buffering data and using FPGA internal RAMs is not efficient at all.

SDRAMs offer a high capacity (up to a number of gigabits) as well as high levels of bandwidth (up to hundreds of Mb/s) for data transmission. The latter one is critical since different modules should be able to access SDRAM at the same time, and the former is essential as the size of injection signal is relatively large and SDRAM should be able to store a huge amount of data. SDRAM's operation is controlled by means of a dedicated memory controller inside the FPGA. Any module requires to access SDRAM's data is connected with memory controller. Using this scheme, the data will be written and read back whenever it is needed. A controller is provided to control the overall operation and manage memory addressing issues.

In order to provide the PC-FPGA connection, Ethernet technology is utilized. The overall architecture of the stack consists of several sub-modules. The physical layer is implemented off-chip using BASE-T standard. Marvell Alaska PHY device is used as an interface for Ethernet communications at 10,100 or 1000 Mb/s speeds. PHY connection to upper layers could be managed through GMII interface which is defined by IEEE802.3 specification. When using GMII, the FPGA designer should consider a logic circuit built in FPGA IO blocks to meet timing requirement [11]. The second layer of the stack is designed using TEMAC (Tri-mode Ethernet MAC) core, two FIFOs and other peripheral circuits and a UDP core comprising of two independent units, the transmitter and receiver units in order to manage incoming and outgoing bytes.

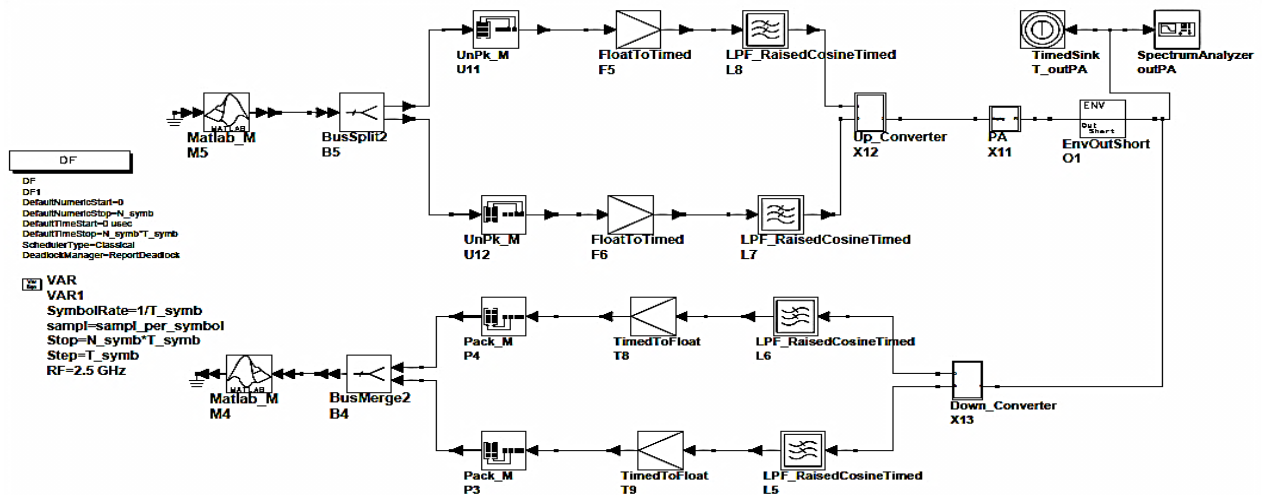


Fig. 1. Schematic of the designed system for simulation purpose

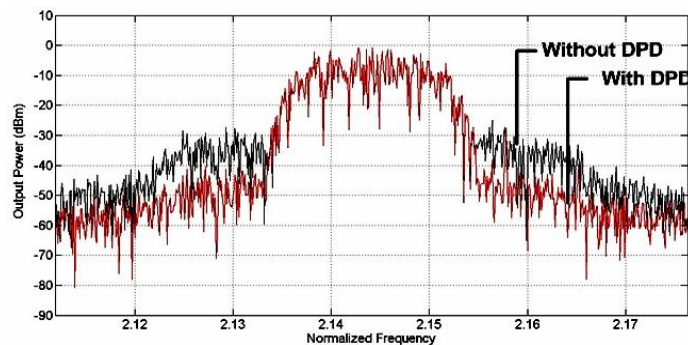


Fig. 2. Output spectrums for 16QAM

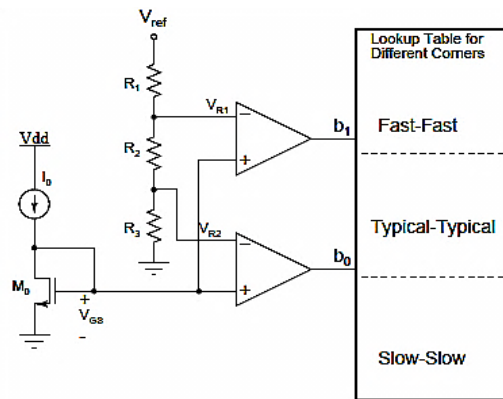


Fig. 3. A circuit to choose the best injection signal

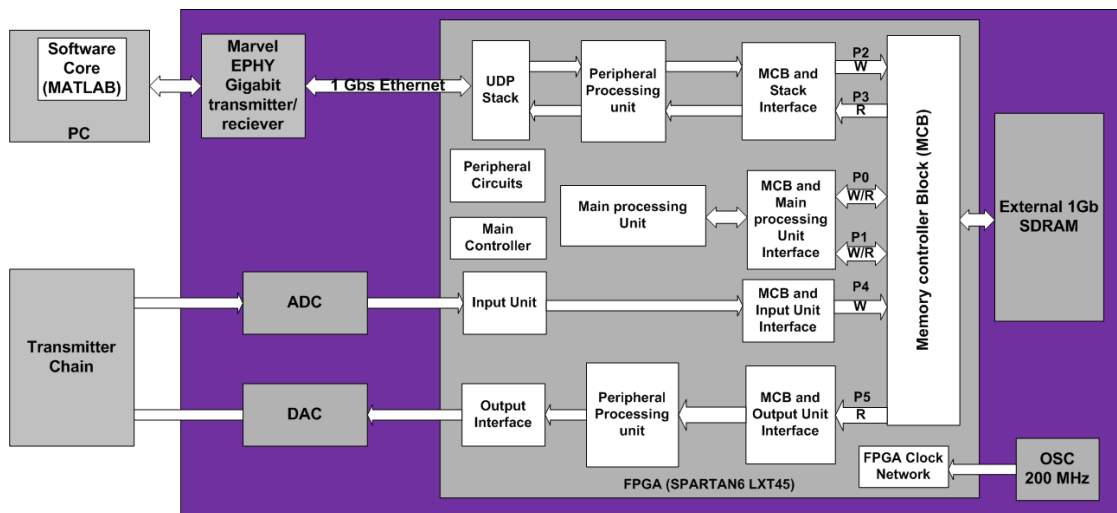


Fig. 4. Overall Architecture of Proposed System

Memory controller block (MCB) is a dedicated embedded block; a multi-port memory controller that simplifies the task of interfacing FPGA devices to the most popular memory standards. In the proposed architecture, the MCB is fed with a 400 MHz differential clock. In addition, 3 unidirectional and 2 bidirectional 32-bit ports configuration is established accompanying with an arbitration scheme which maximizes the performance. A PLL is employed to supply this block with the memory system clock and the calibration clock. Each module that aims to access the external RAM is required to burst a command. In each of the system memory clock cycle (i.e. 3000 Ps), MCB checks the availability of any command in each port's command FIFO based on the arbitration priority. Depend on the burst length of that command and FIFO statuses, data will be transferred.

MCB Interface blocks are units through which the memory controller is accessed. Two MCB Ethernet interface blocks are considered in the design scheme; one is to buffer the incoming Ethernet data packets into the external SDRAM and the other is to fetch data from external RAM and send it over Ethernet to the PC. The architecture is simple and efficient. Writing the incoming data directly into the DDR3 via MCB is quite inefficient since this may waste a significant portion of MCB's bandwidth; hence, when using the system in full operation, achieving real-time operation will be not practical. In order to avoid this, data which is fetched from Ethernet stack is first buffered in an interface FIFO with independent write and read clocks. Peripheral circuits are required for controlling the whole operation. The Output-MCB interface is designed based on two main units. One module is directly connected to the MCB and is responsible for reading injection signal from the SDRAM while the other one consists of

sub-circuits designed mainly for controlling output interface synchronization signals, communicating with the DAC and handshaking with former module.

The designed hardware consumes a negligible area of a Spartan-6 LXT45 Xilinx FPGA. The effectiveness of the system was evaluated by means of both place and route simulation and practical implementation of FPGA design on Spartan-6 LXT45 Xilinx FPGA. Xilinx Integrated Software Environment, ISim and ChipScope analyzer were used for implementation, simulation and debugging purposes respectively. The resource utilization ratio of the whole system is provided in Table. I. The amount of improvement in ACPR of the PA by using predistortion injection technique in this work has been compared with several other methods used in some previous works in Table II which is comparable.

TABLE I: UTILIZATION RATIO

DSP48A1	1	58
PLL_ADV	1	4
MCB	1	2
DCM/DCM_CLKGENS	1	8
RAMB8BWERS	2	232
RAMB16BWERS	8	116
Bonded IOBS	101	296
Slice LUT	2531	27288
Slice Reg	2460	54576
Block	Utilization	Available

TABLE II: COMPARISON OF DIFFERENT METHODS

Reference	[5]	[7]	[9]	[12]	Proposed
Method	Iterative injection	Difference frequencies	First iterative injection	Second harmonics	Third order Inter-modulation
Modulation	EDGE	PHS	16QAM	WCDMA	QPSK
ACPR improvement	10	15.6	15	15	26

conclusion

An efficient injection technique has been proposed in this paper. The technique is based on injection of a digital signal added to the baseband input signal in order to eliminate the intermodulation distortion of the PA. The presented method works successfully for both two tone and wideband input signals. The proposed technique improves nonlinear effects in such a way that the PA could operate effectively up to near saturation without needing any extra RF circuit or analogue elements or feedback loop. This is promising in terms of cost and power consumption. In addition, an FPGA-based system is also proposed in order to solve the technical issues with implementation of the digital predistortion system. MATLAB feeds the injection signal to the FPGA and its associated SDRAM and then, the FPGA is responsible for providing the baseband injected signal to the transmitter chain. Significant improvement in preventing spectral regrowth and reduction in ACPR for different types of modulated signals such as 16QAM, 64QAM and QPSK has been achieved as discussed in the paper.

References

- [1] Ahmed, Asif. "Feedback Linearization of RF Power Amplifier for TETRA Standard," *Bulletin of Electrical Engineering and Informatics* 3, no. 3, 2014.
- [2] Y. K. G. Hau, V. Postoyalko, and J. R. Richardson, "Design and characterization of a microwave feed-forward amplifier with improved wide-band distortion cancellation," *IEEE Transactions on Microwave Theory and Techniques*, vol. 49, no. 1, pp. 200-203, 2001.
- [3] Y. Huang, et al, "Compact wideband linear CMOS variable gain amplifier for analog-predistortion power amplifiers," *IEEE Transactions on Microwave Theory and Techniques*, vol 60, 2012.
- [4] P.L. Gilabert, et al., "Multi-lookup table FPGA implementation of an adaptive digital predistorter for linearizing RF power amplifiers with memory effects," *IEEE Transactions on Microwave Theory and Techniques*, vol. 56, no.2, pp.372-384, Feb. 2008.
- [5] D. Bondar "Linearization of high-efficiency power amplifiers using digital baseband predistortion with iterative injection," *Radio and Wireless Symposium (RWS)*, 2010 IEEE, pp. 148-151. IEEE, 2010.
- [6] Singh, J. E. Scharer, J. H. Booske, and J. G. Wohlbiel, "Second- and third-order signal predistortion for nonlinear distortion suppression in a TWT," *IEEE Transactions on Electron Devices*, vol. 52, issue 5, pp. 709-717, 2005.
- [7] Leung, and M. Cheng, "A new approach to amplifier linearization by the generalized baseband signal injection method," *IEEE Microwave and Wireless Components Letters*, vol. 12, 2002.
- [8] M. Modeste, et al "Analysis and practical performance of a difference frequency technique for improving the multicarrier IMD performance of RF amplifiers," *Technologies for Wireless Applications*, 1999. Digest. 1999 IEEE MTT-S Symposium on, pp. 53-56, 1999.
- [9] M. Xiao, and P. Gardner, "Digital baseband injection techniques to reduce spectral regrowth in power amplifier," *Microwave Symposium Digest, IEEE MTT-S International*, pp. 1513-1516, 2008.
- [10] M.R. Mahmoodi, H. Nikaein, and Z. Fahimi, "A parallel architecture for high speed BLAST using FPGA." *Electrical Engineering (ICEE)*, 2014 22nd Iranian Conference on. IEEE, 2014.
- [11] M.R. Mahmoodi, S.M. Sayedi, and B. Mahmoodi, "Reconfigurable hardware implementation of gigabit UDP/IP stack based on spartan-6 FPGA," In *Information Technology and Electrical Engineering*, International Conference on , vol., no., pp.1-6, 7-8 Oct. 2014
- [12] H. Koulouzis, and D. Budimir, "Distortion correction of LDMOS power amplifiers using hybrid RF second harmoninjection/digital predistortion linearization," *Electrotechnical Conference, MELECON, IEEE Mediterranean*, pp. 177-179, 2006.